

# protein phosphatase 2A catalytic subunit, alpha isoform (PPP2CA) : Time behavioural study of 3rd order combinations in WNT3A stimulated HEK 293 cells

shriprakash sinha

*Independent Researcher; Orcid ID : [orcid.org/0000-0001-7027-5788](https://orcid.org/0000-0001-7027-5788)*

*Address : 104-Madhurisha Heights Phase I, Risali, Bhilai-490006, India*

*Corresponding author email : [sinha.shriprakash@yandex.com](mailto:sinha.shriprakash@yandex.com)*

---

## Abstract

PPP2CA encodes the phosphatase 2A catalytic subunit and is one of the four major Serine/threonine-protein phosphatases. It consists of a common heteromeric core enzyme, composed of a catalytic subunit and a constant regulatory subunit, that associates with a variety of regulatory subunits and it is implicated in the negative control of cell growth and division. Gujral and MacBeath [1] provides a quantitative, and dynamic study of WNT3A-mediated stimulation of HEK 293 cells, where they record time based expression profiles of several response genes which correlated significantly with proliferation and migration. By monitoring the dynamics of gene expression using self-organizing maps, they identified clusters of genes that exhibit similar expression dynamics and uncovered previously unrecognized positive and negative feedback loops. However, their study depicts/uses singular measurements of individual gene expression at different time snapshots/points to infer the system wide analysis of the pathway. At any particular time point, it is often the case that genes are working synergistically in combinations, even though their expression measurements are singular in nature. Here, I • enumerate and rank all 2415 PPP2CA related 3rd order combinations in a forest of  ${}^{71}C_3$  combinations using four different sensitivity methods; • show the conserved rankings for PPP2CA-X-X combinations, which point to existence of biological synergy of some of these combinations across the different sensitivity methods; and • study the behaviour of some of these combinations related to WNT3A response genes that are ranked by the machine learning search engine (Sinha [2]) in time. Patterns of combinations emerge, some of which have been tested in wet lab, while others require further wet lab analysis.

**Keywords:** Sensitivity analysis, Support vector ranking, Hilbert Schmidt Independence Criterion indices (HSIC) and Sobol indices, WNT3A

---

<sup>☆</sup>Time behavioural study of 3-odr PPP2CA comb. in WNT3A stimulated cells

<sup>1</sup>Aspects of unpublished work were presented in a poster session at Cell Symposia: Technology. Biology. Data Science, 9-11 October 2016, Berkeley, California, USA.

---

## 1. Significance

Sinha [2] recently demonstrated the use of machine learning based search engine to rank/reveal gene combinations at 2nd order for the time series data by Gujral and MacBeath [1] and showed how it is possible to locate combinations of priority that might be working synergistically, using sensitivity methods and powerful support vector ranking algorithm. However, the problem explodes combinatorially with even a small set of 71 recorded genes in the study by Gujral and MacBeath [1], when one steps to explore 3rd order combinations. With the total number of  ${}^{71}C_3 (= 57155)$  combinations, it becomes nearly impossible for any biologist to study the system wide dynamics of any pathway. Also, the amount of time usually needed to search for and test a combination is far more than the search done by the machine learning based search engine. Here, I extend the research work by Sinha [2] to conduct a behavioral study of 3rd order PPP2CA related combinations using individual gene expressions measured in time, in WNT3A stimulated HEK 293 cells.

## 2. Introduction

The details of the machine learning based search engine has been recently published in Sinha [2] and deployed to explore the 2nd order combinations of genes in the data set provided by Gujral and MacBeath [1]. Nevertheless, here, I point to the fundamentals of the published work for completeness.

### 2.1. A combinatorial problem

Sensitivity analysis plays a major role in computing the strength of the influence of involved factors in any phenomena under investigation. When applied to expression profiles of various intra/extracellular factors that form an integral part of a signaling pathway, the variance and density based analysis yields a range of sensitivity indices for individual as well as various combinations of factors. These combinations denote the higher order interactions among the involved factors. Computation of higher order interactions is often time consuming but it gives a chance to explore the various combinations that might be of interest in the working mechanism of the pathway. For example, in a range of fourth order combinations among the various factors of the Wnt pathway, it would be easy to assess the influence of the destruction complex formed by APC, AXIN, CSKI and GSK3 interaction. But the effect of these combinations vary over time as measurements of fold changes and deviations in fold changes vary. So it is imperative to know how an interaction or a combination of the involved factors behave in time and Sinha [2] develops a procedure to track the behaviour by exploiting the influences of these involved factors.

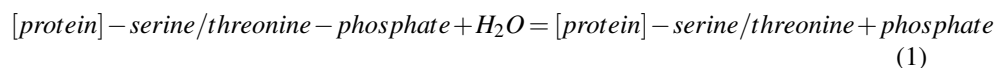
## 2.2. A possible solution

In this work, after estimating the individual effects of factors for a higher order combination, the individual indices are considered as discriminative features. A combination, then, is a feature set in higher order ( $\geq 2$ , i.e. multivariate). With an excessively large number of factors involved in the pathway, it is difficult to search for important combinations in a wide search space over different orders. Exploiting the analogy with the issues of prioritizing webpages using ranking algorithms, for a particular order, a full set of combinations of interactions can then be prioritized based on these features using a powerful ranking algorithm via support vectors Joachims [3]. Recording the changing rankings of the combinations over time reveals how higher order interactions behave within the pathway and when an intervention might be necessary to influence the interaction within the pathway.

## 2.3. protein phosphatase 2A catalytic subunit, alpha isoform (PPP2CA)

Protein phosphorylation is a reversible protein posttranslational modification (PTM). Phosphorylation involves the transfer of phosphate groups from ATP to the enzyme, the energy for which comes from hydrolysing ATP into ADP or AMP. Protein kinases (PKs) are the effectors of phosphorylation and catalyse the transfer of a  $\gamma$ -phosphate from ATP to specific amino acids on proteins. Proteins are phosphorylated predominantly on Ser, Thr and Tyr residues. In contrast, protein phosphatases (PPs) are the primary effectors of dephosphorylation and can be grouped into three main classes based on sequence, structure and catalytic function. Dephosphorylation releases phosphates into solution as free ions, because attaching them back to ATP would require energy input.

PPP2CA is one of the four major serine/threonine-protein phosphatases. Shi [4] studied the mechanism through structure of the serine/threonine phosphatases. The enzyme protein serine/threonine phosphatase acts upon phosphorylated serine/threonine residues as follows (from Wikipedia contributors [5]) :



Jones et al. [6] localized the the gene for the  $\alpha$  isoform of the catalytic subunit of human PPP2CA to chromosome 5 using somatic cell hybrids, and then more finely mapped to chromosome region 5q23– >q31 by in situ hybridization using a tritiated cDNA probe. In their review, Seshacharyulu et al. [7] focus on the structural complexity of serine/threonine phosphatase PP2A and summarize its expression pattern in cancer while discussing about the PP2A interacting and regulatory proteins and substrates. Finally, they also review the mouse models developed to understand the biological role of PP2A subunits in an in vivo model system. Further, Reynhout and Janssens [8] summarize current knowledge on physiologic functions of PP2A in germ cell maturation, tumor suppression, metabolic regulation, embryonic development, and homeostasis of adult brain, liver, heart, immune system, lung, kidney, intestine, skin, eye and bone, all of which were retrieved from in vivo studies using PP2A transgenic, knockout or knockin mice.

The phosphatases PP1 and PP2A catalytic subunits exist in cells in form of holoenzymes, which impart substrate specificity and their contribution to the recognition of substrates is unclear. Hoermann et al. [9] develop a phosphopeptide library approach and a phosphoproteomic assay to demonstrate that the specificity of PP1 and PP2A holoenzymes towards pThr and of PP1 for basic motifs adjacent to the phosphorylation site are due to intrinsic properties of the catalytic subunits.

PP2A holoenzyme complex comprises a scaffolding (A), regulatory (B), and catalytic (C) subunit, with PPP2CA being the principal catalytic subunit. To define the full scope of PP2A substrates in cells, Brewer et al. [10] employed dTAG proteolysis-targeting chimeras to efficiently and selectively degrade dTAG-PPP2CA in homozygous knock-in HEK293 cells. Via unbiased global phospho-proteomics, they identified 2,204 proteins with significantly increased phosphorylation upon dTAG-PPP2CA degradation, implicating them as potential PPP2CA substrates and through bioinformatic analyses, they revealed involvement of the potential PPP2CA substrates in spliceosome function, cell cycle, RNA transport, and ubiquitin-mediated proteolysis. Using quantitative phospho-proteomic analysis, they identified a total of 39,103 phosphopeptides belonging to 5,829 proteins, in DMSO- and dTAG-13-treated <sup>dTAG/dTAG</sup>PPP2CA HEK293 cell extracts. Of these, 2,651 phospho-peptides corresponding to 1,149 proteins showed a significant increase in abundance of >2-fold in dTAG-13-treated cells compared to DMSO-treated controls, while 6,280 phospho-peptides corresponding to 2,204 proteins showed a significant increase in abundance of >1.5-fold.

I present 3rd order combinations of PPP2CA with other genes, that the machine learning based search engine points to, as possible synergistic combinations that might be working in time.

### 3. Methods

Please refer to sections of Sinha [2] for methods, design of study and analysis of data for 2nd order combinations. The same method and design of study is used to generate results for 3rd order combinations presented in this study.

### 4. Time series data

Gujral and MacBeath [1] present a set of 71 WNT-related gene expression values for 6 different time points over a range of 24-hour period using qPCR. The changes represent the fold-change in the expression levels of genes in 200 ng/mL WNT3A-stimulated HEK 293 cells in time relative to their levels in unstimulated, serum-starved cells at 0-hour. Gujral and MacBeath [1] state that qPCR data are the means of three biological replicates. Only genes whose mean transcript levels changed by more than two-fold at one or more time points during the 24-hour time course were considered significant. Positive (negative) numbers represent up (down) -regulation. We have already covered the issues related to these data sets in detail in Sinha [11]. Readers are requested to go through them in the pointed reference. The tools of study which are used here have been published in another foundational work in Sinha [11].

## 5. Design of experiment

### 5.1. Pipeline for time series data

For the case of time series data, interactions among the contributing factors are studied by comparing triplets of fold-changes at single time points. The procedure begins with the generation of distribution around measurements at single time points with added noise is done to estimate the indices. A distribution is generated for the fold changes at single time points. Then for every gene, there is a vector of values representing fold changes as well as deviations in fold changes for different time points and durations between time points, respectively. Next a listing of all  $C_k^n$  combinations for  $k$  number of genes from a total of  $n$  genes is generated.  $k$  is  $\geq 2$  and  $\leq (n - 1)$ . Each of the combination of order  $k$  represents a unique set of interaction between the involved genetic factors. After this, the datasets are combined in a specified format which go as input as per the requirement of a particular sensitivity analysis method. Thus for each  $p^{th}$  combination in  $C_k^n$  combinations, the dataset is prepared in the required format from the distributions for two separate cases which have been discussed above. (See .R code in mainScript-1-1.R). After the data has been transformed, vectorized programming is employed for density based sensitivity analysis and looping is employed for variance based sensitivity analysis to compute the required sensitivity indices for each of the  $p$  combinations. This procedure is done for different kinds of sensitivity analysis methods.

After the above sensitivity indices have been stored for each of the  $p^{th}$  combination, the next step in the design of experiment is conducted. Since there is only one recording of sensitivity index per combination, each combination forms a training example which is allotted a training index and the sensitivity indices of the individual genetic factors form the training example. Thus there are  $C_k^n$  training examples for  $k^{th}$  order interaction. Using this training set  $SVM_{learn}^{Rank}$  Joachims [3] is used to generate a model on default value  $C$  value of 20. In the current experiment on toy model  $C$  value has not been tuned. The training set helps in the generation of the model as the different gene combinations are numbered in order which are used as rank indices. The model is then used to generate score on the observations in the testing set using the  $SVM_{classify}^{Rank}$  Joachims [3]. Note that due to availability of only one example per combination, after the model has been built, the same training data is used as test data to generate the scores. This procedure is executed for each and every sensitivity analysis method. This is followed by sorting of these scores along with the rank indices (i.e the training indices) already assigned to the gene combinations. The end result is a sorted order of the gene combinations based on the ranking score learned by the  $SVM^{Rank}$  algorithm. Finally, this entire procedure is computed for sensitivity indices generated for each and every fold change at time point and deviations in fold change at different durations. Observing the changing rank of a particular combination at different times and different time periods will reveal how a combination is behaving.

Note that the following is the order in which the files should be executed in R, in order, for obtaining the desired results (Note that the code will not be explained here) - • use source("mainScript-1-1.R") with arguments for Dynamic data • source("SVMRank-Results-D.R"), to rank the interactions (again this needs to be done separately for

different kinds of SA methods), • use source("Combine-Time-files.R"), if computing indices separately via previous file, • source("Sort-n-Plot-D.R") to sort the interactions. Note that the sorting changes the interaction ranking in time. Thus • use source("Interaction-Priority-Intime.R") to find the prioritized ranking of each and every interaction over the different time points and finally • use source("Print-Ranking-AND-Interaction-Rank.R") to print individual ranking of the required input factor with other interaction factors.

## 6. Results & Discussion

### 6.1. Time series data by Gujral and MacBeath [1]

NOTE - Ranking was assigned on scores that were sorted in DECREASING values. So, 1 was assigned to highest score and vice versa.

Results for the 3<sup>rd</sup> order interactions are presented here. The results first discuss the behaviour of interactions across the snapshots of time using the computed sensitivities on fold change measurements per time snapshot. The analysis was done using 4 different sensitivity indices. Out of the  $^{71}C_3$  combinations, I consider/present only those combinations that show a ranking within first 10,000 out of 57,155. This choice is liberal and biologists/oncologists can have a more stricter choice as per need. Two observations are made, • the ranking of a particular combination is conserved (i.e within the 10,000 range) in a particular time point or in the early phase or late phase of WNT3A stimulation, across the majority of the four sensitivity methods, which is a strict criteria of assessment or • the ranking of a particular combination is conserved across time points/phase (i.e they are within the 10,000 range) and the majority of the four sensitivity methods, which is relaxed criteria of assessment. Applying this filter helps reveal important combinations of interest that might be working synergistically at a higher order level in the cell.

Regarding technical points of implementation, the rankings were generated without scaling/normalizing the time series data provided by Gujral and MacBeath [1]. For estimating the sensitivity indices, a small gaussian distribution using the function **rnorm** that generates a vector of normally distributed random variables given a vector length n (here 9, the 10th one is the mean/recorded gene regulation itself), a population mean  $\mu$  and population standard deviation  $\sigma$ . The syntax for using rnorm is as follows: **rnorm(n, mean, sd)**. Further, I use the **jitter** function to add a little bit of noise to the data. This helps to see if the generated rankings are robust or not.

### 6.2. Enumeration and ranking of 2415 PPP2CA-X-X combinations from Gujral and MacBeath [1]

In the supplementary section, I present four files, each containing the rankings of 3rd order combinations, that vary in time (shown for 5 time points). Each file represents the rankings computed using a particular sensitivity method. The changing rankings in time for a particular combination represents the importance of contribution/role that combination plays in the cell stimulated with WNT3A. The sensitivity methods used

are Hilbert Schmidt Independence Criterion indices (HSIC) indices (with rbf and linear kernel in Da Veiga [12]) and Sobol indices (with 2002 implementation in Saltelli [13] and martinez implementation in Martinez [14] and Baudin et al. [15]).

### 6.3. Conserved machine learning rankings for tested PPP2CA-X-X combinations

A total of 2415, 3rd order combinations involving PPP2CA were obtained from a full set of  ${}^{71}C_3 = 57155$  combinations. Further, from this selected set, using the above criteria for conserved rankings, I report/tabulate the meaningful combinations that might be working synergistically. Tables 2, 3 and 4 show the rankings for the same combinations as in table 1, but using rbf kernel for HSIC, 2002 implementation for SOBOL and martinez implementation for SOBOL, respectively. As one tallies the rankings of across these tables for a particular combination, one finds that the role of the combination of interest is conserved. This conservation points to the existence of the biological synergy, whether the combination has been tested or unexplored/untested.

#### 6.3.1. Examining the behaviour of AXIN-PPP2CA-X combinations

Willert et al. [16] show that AXIN is dephosphorylated in response to WNT signaling and the dephosphorylated AXIN binds  $\beta$ -catenin less efficiently than the phosphorylated form. Thus, WNT signaling lowered AXIN's affinity for  $\beta$ -catenin, thereby disengaging  $\beta$ -catenin from the degradation machinery. Ikeda et al. [17] show that the heterodimeric form of PP2A directly binds to AXIN, and PP2A complexed with AXIN dephosphorylated APC phosphorylated by GSK3 $\beta$ . Taken together, their results suggest that GSK3 $\beta$ -dependent phosphorylation of APC can be modulated by  $\beta$ -catenin and PP2A complexed with AXIN. Looking at the tables above, one finds the following combinations for AXIN1 along with PPP2CA, to be prominent at 3rd order level - AXIN1-FZD2-PPP2CA, AES-AXIN1-PPP2CA and AXIN1-FOXN1-PPP2CA. All these combinations indicate the existence of a possible synergy when they take a higher rank in the list of combinations.

#### 6.3.2. Examining the behaviour of APC-PPP2CA-X combinations

Seeling et al. [18] show that PP2A regulatory subunit, B56, interacted with APC in the yeast two-hybrid system and expression of B56 reduced the abundance of  $\beta$ -catenin and inhibited transcription of  $\beta$ -catenin target genes in mammalian cells and Xenopus embryo explants. Further, the B56-dependent decrease in  $\beta$ -catenin was blocked by oncogenic mutations in  $\beta$ -catenin or APC, and by proteasome inhibitors. B56 may direct PP2A to dephosphorylate specific components of the APC-dependent signaling complex and thereby inhibit WNT signaling. Their study suggested that PP2A heterotrimer containing the B56 regulatory subunit functioned in the WNT signaling complex to down-regulate  $\beta$ -catenin, perhaps through an interaction of B56 and the NH<sub>2</sub>-terminus of APC, to dephosphorylate specific components of the APC-dependent signaling complex and thereby inhibit WNT signaling. Looking at the tables above,

RANKING @ $t_i$ USING HSIC - LINEAR											
3rd order comb.	$t_1$	$t_3$	$t_6$	$t_{12}$	$t_{24}$	3rd order comb.	$t_1$	$t_3$	$t_6$	$t_{12}$	$t_{24}$
CXXC4-FZD7-PPP2CA	90	9819	23105	12397	36836	FZD7-PPP2CA-SFRP4	121	6838	2610	6467	34834
FZD1-FZD7-PPP2CA	188	20213	26368	10322	10221	AES-AXIN1-PPP2CA	213	21529	16225	49328	28118
CSNK2A1-MYC-PPP2CA	271	37740	40109	23353	26864	APC-PITX2-PPP2CA	334	14753	2900	19245	30663
NLK-PORCN-PPP2CA	339	30605	43435	41734	4166	PPP2CA-SFRP4-WNT2B	341	52722	25356	52978	1988
KREMEN1-PPP2CA-SFRP4	362	833	2893	48271	49787	FZD7-NKD1-PPP2CA	369	8802	35791	35537	25608
DKK1-JUN-PPP2CA	408	27394	50340	28816	37806	BCL9-PORCN-PPP2CA	415	15959	34237	38189	34019
DIXDC1-NKD1-PPP2CA	440	13162	40123	35144	6197	CXXC4-PORCN-PPP2CA	481	22027	38709	38555	36190
DVL2-JUN-PPP2CA	504	43997	37157	2445	3613	FZD7-PPP2CA-SEN2	540	11483	354	3539	34512
CCND3-PPP2CA-SFRP4	631	37304	7579	35575	51606	PPP2CA-WNT1-WNT3A	732	6546	10800	53535	9982
DKK1-PPP2CA-SFRP4	815	3000	44035	44920	42238	FBXW11-LRP6-PPP2CA	822	25174	30818	7903	41062
FSHB-FZD2-PPP2CA	922	15170	15248	37534	18116	CSNK1G1-NKD1-PPP2CA	926	17356	35232	35369	2912
DVL1-FOXN1-PPP2CA	977	25908	15392	4810	48741	DAAM1-FOXN1-PPP2CA	1014	50289	35190	8828	44977
CTBP1-GSK3A-PPP2CA	1015	17069	883	43553	18661	FOSL1-FOXN1-PPP2CA	1072	22257	16994	9632	25457
CSNK1G1-FZD2-PPP2CA	1082	23722	6311	56537	35909	FOSL1-FZD7-PPP2CA	1103	37962	25642	24479	50931
FZD8-GSK3A-PPP2CA	1156	55038	1341	50154	22462	CTNNB1P1-JUN-PPP2CA	1160	17287	25595	27276	6859
CSNK1D-FOXN1-PPP2CA	1252	17427	16752	21509	34632	FBXW11-FOXN1-PPP2CA	1357	8568	16917	13742	17017
FRZB-JUN-PPP2CA	1383	13534	31714	933	1610	CSNK2A1-FOXN1-PPP2CA	1415	18676	25465	10950	9597
PPP2CA-T-WNT3A	1435	46308	13460	20855	21652	FRZB-FZD2-PPP2CA	1437	17024	10096	32430	33434
CSNK1G1-FSHB-PPP2CA	1518	8523	49087	1235	27660	CCND1-JUN-PPP2CA	1525	10554	35624	43398	54711
CSNK2A1-FSHB-PPP2CA	1544	21794	56458	12205	17377	KREMEN1-PPP2CA-WNT2B	1585	14425	197	53141	37098
DKK1-FOXN1-PPP2CA	1604	39842	25588	9674	22711	FRZB-GSK3A-PPP2CA	1624	17689	1801	14917	16232
BTRC-PPP2CA-WNT4	1638	35087	32587	22025	51750	FZD5-CCND3-PPP2CA	1659	15307	15361	43028	36850
PPP2CA-WNT1-WNT4	1668	20515	14866	23920	21265	AES-FOXN1-PPP2CA	1682	1873	24710	15282	25404
FZD8-PORCN-PPP2CA	1713	51044	29439	20913	20485	FZD5-PPP2CA-SFRP4	1743	159	4915	40308	39122
CSNK1A1-LRP6-PPP2CA	1764	14481	17648	2115	28490	FOSL1-NKD1-PPP2CA	1845	14335	40783	24581	23211
FZD7-PPP2CA-WNT2B	1854	16103	178	39687	33132	APC-BTRC-PPP2CA	1858	9257	27876	20401	45249
FOSL1-PORCN-PPP2CA	1917	33808	39279	26918	22451	FRZB-NKD1-PPP2CA	1923	12714	42040	19751	23511
AXIN1-FZD2-PPP2CA	2006	16397	13459	38219	30167	DKK1-PPP2CA-SEN2	2068	7041	27771	41618	51588
CSNK1D-FGF4-PPP2CA	2103	20756	11349	39534	15407	FZD8-JUN-PPP2CA	2138	54751	19454	329	37826
DKK1-NKD1-PPP2CA	2158	21388	52610	49493	9273	CSNK1G1-JUN-PPP2CA	2194	17201	31808	2244	24092
FBXW11-JUN-PPP2CA	2233	16460	49863	18037	53295	FZD6-GSK3A-PPP2CA	2263	8382	9486	47912	53738
FOSL1-GSK3A-PPP2CA	2355	22861	911	45587	39936	DAAM1-LRP6-PPP2CA	2361	55059	33326	5010	40824
CSNK1A1-GSK3B-PPP2CA	2386	9444	19245	4822	2538	BCL9-JUN-PPP2CA	2418	12028	23042	32377	49157
FRZB-PPP2CA-SFRP4	2426	1736	4164	8420	12593	CTBP2-FOXN1-PPP2CA	2521	39676	20597	7309	30523
DKK1-GSK3A-PPP2CA	2529	18354	4501	38825	41214	BCL9-FGF4-PPP2CA	2534	11917	24166	51167	48006
FRAT1-JUN-PPP2CA	2547	32152	28002	1650	1276	APC-PORCN-PPP2CA	2593	14870	33789	20601	17503
CXXC4-FZD2-PPP2CA	2607	29974	9988	18663	50107	FRAT1-GSK3A-PPP2CA	2638	38412	1286	35232	13767
BTRC-PPP2CA-SFRP4	2649	45450	55216	41081	48220	FRZB-PORCN-PPP2CA	2663	20449	38661	30250	22743
EP300-FZD2-PPP2CA	2702	12448	13262	50046	20911	DAAM1-GSK3A-PPP2CA	2745	56040	14776	51085	48063
CCND3-PPP2CA-WNT2	2799	33277	2300	17044	49518	FBXW2-NKD1-PPP2CA	2839	23721	34814	16169	56279
PITX2-PORCN-PPP2CA	2847	24874	33030	43172	21878	CTBP1-FOXN1-PPP2CA	2940	12144	24777	14758	54034
FZD7-PPP2CA-WNT2	2964	18295	2936	723	46075	CCND3-PPP2CA-SEN2	3064	34905	2328	40674	48547
PPP2CA-WNT1-WNT5A	3127	17958	20275	50785	22700	AXIN1-FOXN1-PPP2CA	3158	9114	17327	16618	10071
NKD1-PPP2CA-SFRP4	3169	46409	13326	29656	43339	FGF4-FOSL1-PPP2CA	3175	29507	37541	48577	51007
AES-EP300-PPP2CA	3218	22740	43678	26060	41565	CTBP1-FGF4-PPP2CA	3224	17798	20777	35300	21473
DIXDC1-FOXN1-PPP2CA	3235	4976	13715	8671	2172	APC-FOXN1-PPP2CA	3259	6614	11418	7307	27730
CXXC4-FOXN1-PPP2CA	3277	19301	19575	24116	33763	CCND3-NKD1-PPP2CA	3285	34449	42225	49257	26308
GSK3B-LRP6-PPP2CA	3297	38834	21470	36021	39453	FOSL1-JUN-PPP2CA	3303	25232	24882	2685	4764
FBXW11-FZD2-PPP2CA	3313	19812	19095	30619	15139	FOSL1-PPP2CA-SFRP4	3331	18404	4076	19432	6798
CXXC4-FGF4-PPP2CA	3340	9402	29074	35299	53290	CCND1-NKD1-PPP2CA	3363	11274	37598	54652	44854
PPP2CA-TCF7-WNT3A	3403	35126	15557	53522	39901	FBXW2-PORCN-PPP2CA	3520	27173	22022	46128	27903
AES-DVL1-PPP2CA	3635	6018	44845	39717	52837	CXXC4-JUN-PPP2CA	3661	32213	26859	462	30021
DIXDC1-FZD2-PPP2CA	3662	17928	10686	40372	29250	DAAM1-FGF4-PPP2CA	3665	54152	33362	55780	29602
FZD8-NKD1-PPP2CA	3681	49836	33279	27543	15965	APC-FZD6-PPP2CA	3769	15339	20803	56646	49253
FZD6-PORCN-PPP2CA	3788	4773	43421	3483	7109	BTRC-PPP2CA-T	3795	43011	19216	31904	44253
FBXW11-GSK3A-PPP2CA	3852	26830	8953	53718	5344	FZD5-PORCN-PPP2CA	3939	10638	39482	21947	53216
CSNK2A1-NKD1-PPP2CA	4025	15782	45180	27270	33423	CSNK1D-GSK3A-PPP2CA	4064	22624	794	37163	9946
DIXDC1-PITX2-PPP2CA	4123	13781	1911	14325	45522	DKK1-DVL2-PPP2CA	4138	22771	24516	8573	52303
FZD8-LEF1-PPP2CA	4177	56827	23717	17918	45636	FRAT1-PORCN-PPP2CA	4204	33092	39327	31761	14446
CCND3-PPP2CA-RHOU	4207	37434	5715	53381	50362	CSNK2A1-GSK3A-PPP2CA	4214	31336	13790	24722	34871
PPP2CA-WNT1-WNT2B	4221	27679	5501	15908	49412	FZD1-PORCN-PPP2CA	4258	20050	38961	32098	15000
FZD7-PPP2CA-TLE2	4271	5239	7231	4827	26456	CTNNB1-GSK3A-PPP2CA	4281	19241	845	32420	18538
CCND1-CTNNB1P1-PPP2CA	4294	35830	34555	37986	51377	KREMEN1-PPP2CA-SEN2	4308	6165	521	42127	55415

Table 1: Rankings of PPP2CA-X-X. A list of approximately first 125 combinations with rankings below 10,000 out of 57,155. SA - HSIC; Kernel - linear

one finds the following combinations for AXIN1 along with PPP2CA, to be prominent at 3rd order level - APC-PITX2-PPP2CA, APC-BTRC-PPP2CA, APC-PORCN-PPP2CA, APC-FOXN1-PPP2CA and APC-FZD6-PPP2CA . All these combinations indicate the existence of a possible synergy when they take a higher rank in the list of



RANKING @ $t_i$ USING HSIC - RBF												
3rd order comb.	$t_1$	$t_3$	$t_6$	$t_{12}$	$t_{24}$	3rd order comb.	$t_1$	$t_3$	$t_6$	$t_{12}$	$t_{24}$	
CXXC4-FZD7-PPP2CA	7569	8146	8359	8809	29695	FZD7-PPP2CA-SFRP4	55917	24461	55999	42034	109	
FZD1-FZD7-PPP2CA	25993	15034	5386	38356	42649	AES-AXIN1-PPP2CA	35492	17204	7775	30194	15980	
CSNK2A1-MYC-PPP2CA	1074	26347	29622	32938	20490	APC-PITX2-PPP2CA	4042	33446	8698	18579	52910	
NLK-PORCN-PPP2CA	6640	37879	19229	30844	45007	PPP2CA-SFRP4-WNT2B	55580	46429	27467	46270	1672	
KREMEN1-PPP2CA-SFRP4	19893	13395	43502	13961	6353	FZD7-NKD1-PPP2CA	15127	35957	31673	37533	1778	
DKK1-JUN-PPP2CA	872	31181	33266	21737	30431	BCL9-PORCN-PPP2CA	19443	12204	3989	2860	44188	
DIXDC1-NKD1-PPP2CA	9807	43231	37477	30170	1078	CXXC4-PORCN-PPP2CA	9663	20715	7491	12348	51537	
DVL2-JUN-PPP2CA	12969	55374	21200	14940	32734	FZD7-PPP2CA-SEN2	32571	2154	49346	21000	26293	
CCND3-PPP2CA-SFRP4	46916	36878	55760	47246	5936	PPP2CA-WNT1-WNT3A	4487	6874	35552	24125	19493	
DKK1-PPP2CA-SFRP4	55812	1395	43571	11747	8786	FBXW11-LRP6-PPP2CA	1498	23055	36283	10416	6272	
FSHB-FZD2-PPP2CA	3195	15838	9446	3827	55246	CSNK1G1-NKD1-PPP2CA	8799	37693	42013	33688	15900	
DVL1-FOXN1-PPP2CA	3346	22402	46063	15109	11834	DAAM1-FOXN1-PPP2CA	609	47634	41711	1552	16742	
CTBP1-GSK3A-PPP2CA	841	30822	34980	31747	27039	FOSL1-FOXN1-PPP2CA	2050	20570	56654	7068	31115	
CSNK1G1-FZD2-PPP2CA	21192	37740	25191	13344	44898	FOSL1-FZD7-PPP2CA	54451	46826	3194	28518	28447	
FZD8-GSK3A-PPP2CA	2976	56637	43724	15698	9354	CTNNB1P1-JUN-PPP2CA	38196	36635	20141	33944	38991	
CSNK1D-FOXN1-PPP2CA	677	25144	54449	26225	44186	FBXW11-FOXN1-PPP2CA	551	13483	50027	13549	5121	
FRZB-JUN-PPP2CA	5873	49297	3845	20493	26715	CSNK2A1-FOXN1-PPP2CA	278	35287	48412	13705	23060	
PPP2CA-T-WNT3A	5197	44818	17755	38317	4985	FRZB-FZD2-PPP2CA	5746	32562	6231	841	53357	
CSNK1G1-FSHB-PPP2CA	50070	6934	23453	5427	21042	CCND1-JUN-PPP2CA	40595	14062	3971	9088	1571	
CSNK2A1-FSHB-PPP2CA	14473	24470	49869	6189	28547	KREMEN1-PPP2CA-WNT2B	25164	28694	34566	35971	17687	
DKK1-FOXN1-PPP2CA	318	42768	43072	5776	28884	FRZB-GSK3A-PPP2CA	1260	45624	46852	17140	25632	
BTRC-PPP2CA-WNT4	13782	33555	41012	5416	5243	FZD5-CCND3-PPP2CA	12325	45904	23439	31013	47189	
PPP2CA-WNT1-WNT4	1316	18383	42717	1659	16550	AES-FOXN1-PPP2CA	2186	37914	47459	13594	25139	
FZD8-PORCN-PPP2CA	4402	55143	2005	12002	37055	FZD5-PPP2CA-SFRP4	47311	664	55943	2216	11593	
CSNK1A1-LRP6-PPP2CA	16978	31404	24202	26610	21103	FOSL1-NKD1-PPP2CA	21934	29546	42661	35675	17456	
FZD7-PPP2CA-WNT2B	54842	24004	41817	52487	4145	APC-BTRC-PPP2CA	4261	9237	29395	1410	54704	
FOSL1-PORCN-PPP2CA	857	51996	6161	7188	48966	FRZB-NKD1-PPP2CA	1942	36043	22753	20309	35265	
AXIN1-FZD2-PPP2CA	7416	35245	5191	10583	50255	DKK1-PPP2CA-SEN2	54622	26587	44748	26854	52986	
CSNK1D-FGF4-PPP2CA	3187	47005	13018	23779	39413	FZD8-JUN-PPP2CA	6710	57073	4320	19608	19584	
DKK1-NKD1-PPP2CA	845	43108	38644	15851	21492	CSNK1G1-JUN-PPP2CA	3740	31530	16470	29436	25461	
FBXW11-JUN-PPP2CA	9373	17254	50937	17677	11233	FZD6-GSK3A-PPP2CA	5274	18421	36558	40884	12260	
FOSL1-GSK3A-PPP2CA	12185	33599	52257	41997	37270	DAAM1-LRP6-PPP2CA	7255	52778	39048	19324	16287	
CSNK1A1-GSK3B-PPP2CA	49785	6326	16521	6418	41571	BCL9-JUN-PPP2CA	32542	20885	2900	20877	26335	
FRZB-PPP2CA-SFRP4	52697	31347	51732	14973	22371	CTBP2-FOXN1-PPP2CA	11045	38092	52532	1356	32277	
DKK1-GSK3A-PPP2CA	55	13432	43272	11984	17851	BCL9-FGF4-PPP2CA	11758	12541	2912	24152	44954	
FRAT1-JUN-PPP2CA	5774	39371	22955	20982	28298	APC-PORCN-PPP2CA	1049	35875	5774	24955	45838	
CXXC4-FZD2-PPP2CA	11564	33338	12458	3001	54858	FRAT1-GSK3A-PPP2CA	761	45444	39194	15449	37603	
BTRC-PPP2CA-SFRP4	23701	47316	54163	28713	3631	FRZB-PORCN-PPP2CA	4450	31541	6488	11176	47491	
EP300-FZD2-PPP2CA	8059	21295	864	5359	44323	DAAM1-GSK3A-PPP2CA	5817	54945	44951	39069	16387	
CCND3-PPP2CA-WNT2	36713	24526	54134	13742	8094	FBXW2-NKD1-PPP2CA	15124	44885	17926	12733	2217	
PITX2-PORCN-PPP2CA	9603	23189	295	19554	39138	CTBP1-FOXN1-PPP2CA	5258	32520	39917	10063	30654	
FZD7-PPP2CA-WNT2	40336	26902	57064	15776	2793	CCND3-PPP2CA-SEN2	42453	28981	45394	1751	13534	
PPP2CA-WNT1-WNT5A	1188	16609	32224	18050	32772	AXIN1-FOXN1-PPP2CA	5167	25187	29990	1127	16140	
NKD1-PPP2CA-SFRP4	40324	48641	51898	9183	19710	FGF4-FOSL1-PPP2CA	42277	28170	8091	25442	19223	
AES-EP300-PPP2CA	40675	14926	3496	32198	22117	CTBP1-FGF4-PPP2CA	3823	27672	4141	30441	47610	
DIXDC1-FOXN1-PPP2CA	1796	26077	33448	2622	1308	APC-FOXN1-PPP2CA	1206	4752	36187	915	15627	
CXXC4-FOXN1-PPP2CA	1922	14941	49768	109	32177	CCND3-NKD1-PPP2CA	19772	35706	47585	36014	3731	
GSK3B-LRP6-PPP2CA	3750	50098	25527	8818	33308	FOSL1-JUN-PPP2CA	21063	49029	6511	48244	44672	
FBXW11-FZD2-PPP2CA	3595	19254	48774	3116	27274	FOSL1-PPP2CA-SFRP4	31966	44588	53340	39850	33169	
CXXC4-FGF4-PPP2CA	896	24972	12137	33837	43059	CCND1-NKD1-PPP2CA	31094	31919	45839	10804	5523	
PPP2CA-TCF7-WNT3A	36467	12019	36560	49458	39632	FBXW2-PORCN-PPP2CA	13731	19973	12814	22383	21062	
AES-DVL1-PPP2CA	19128	12832	8371	36154	55869	CXXC4-JUN-PPP2CA	2697	40480	12704	20114	45550	
DIXDC1-FZD2-PPP2CA	8902	30326	5894	8118	11004	DAAM1-FGF4-PPP2CA	1734	53041	30385	36043	10689	
FZD8-NKD1-PPP2CA	31727	55399	17443	4434	10950	APC-FZD6-PPP2CA	9255	28099	28345	32780	55276	
FZD6-PORCN-PPP2CA	15	24063	29679	24492	40813	BTRC-PPP2CA-T	42753	54274	45558	42965	26218	
FBXW11-GSK3A-PPP2CA	5045	19409	45810	19725	16426	FZD5-PORCN-PPP2CA	23568	21263	11481	8780	45819	
CSNK2A1-NKD1-PPP2CA	6422	22743	30647	42195	19402	CSNK1D-GSK3A-PPP2CA	1046	40897	47094	14850	34061	
DIXDC1-PITX2-PPP2CA	5166	50281	13595	5982	18374	DKK1-DVL2-PPP2CA	2732	42296	39816	1658	9495	
FZD8-LEF1-PPP2CA	4960	57112	5320	15616	6681	FRAT1-PORCN-PPP2CA	2795	32747	21472	22562	46364	
CCND3-PPP2CA-RHOU	24349	40806	49185	54625	8752	CSNK2A1-GSK3A-PPP2CA	8360	44268	37323	48745	27502	
PPP2CA-WNT1-WNT2B	5623	15143	40493	2300	24871	FZD1-PORCN-PPP2CA	4367	38671	4743	23669	51214	
FZD7-PPP2CA-TLE2	56558	28223	50599	11481	3392	CTNNB1-GSK3A-PPP2CA	2288	19240	46473	33276	26230	
CCND1-CTNNB1P1-PPP2CA	9077	28086	5722	5046	6609	KREMEN1-PPP2CA-SEN2	3092	4451	26948	15879	51552	

Table 2: Rankings of PPP2CA-X-X. A list of approximately first 125 combinations with rankings below 10,000 out of 57,155. SA - HSIC; Kernel - rbf

combinations.

RANKING @ $t_1$ USING SOBOL - 2002												
3rd order comb.	$t_1$	$t_3$	$t_6$	$t_{12}$	$t_{24}$	3rd order comb.	$t_1$	$t_3$	$t_6$	$t_{12}$	$t_{24}$	
CXXC4-FZD7-PPP2CA	6148	28592	25213	26202	44025	FZD7-PPP2CA-SFRP4	4427	6241	20755	12790	56870	
FZD1-FZD7-PPP2CA	12964	30861	23477	9052	52864	AES-AXIN1-PPP2CA	44475	32683	37476	33250	13231	
CSNK2A1-MYC-PPP2CA	13455	56732	1328	24242	47656	APC-PITX2-PPP2CA	24251	10201	10127	26604	27627	
NLK-PORCN-PPP2CA	2376	11307	5767	13480	29665	PPP2CA-SFRP4-WNT2B	45917	16377	56750	51527	8872	
KREMEN1-PPP2CA-SFRP4	47389	38291	46157	33295	21478	FZD7-NKD1-PPP2CA	9005	18778	1246	2338	53443	
DKK1-JUN-PPP2CA	98	19110	16349	21529	30627	BCL9-PORCN-PPP2CA	50172	47074	50265	53138	6075	
DIXDC1-NKD1-PPP2CA	13275	33550	23785	28183	10803	CXXC4-PORCN-PPP2CA	13026	53831	3318	18245	41235	
DVL2-JUN-PPP2CA	24259	24689	15208	7592	48248	FZD7-PPP2CA-SEN2	10937	22503	18140	21817	45345	
CCND3-PPP2CA-SFRP4	43208	48312	31466	42666	24948	PPP2CA-WNT1-WNT3A	40524	9682	46210	50633	28358	
DKK1-PPP2CA-SFRP4	48919	16498	41484	28920	14943	FBXW11-LRP6-PPP2CA	23575	5282	15764	15190	57017	
FSHB-FZD2-PPP2CA	15048	34207	8473	13799	49835	CSNK1G1-NKD1-PPP2CA	2818	12720	1066	16639	39238	
DVL1-FOXN1-PPP2CA	5338	52223	20041	27389	38036	DAAM1-FOXN1-PPP2CA	21001	49584	22517	19252	54625	
CTBP1-GSK3A-PPP2CA	33646	44504	35935	37378	26248	FOSL1-FOXN1-PPP2CA	51329	15073	48971	51617	23899	
CSNK1G1-FZD2-PPP2CA	7371	1821	2940	12583	54147	FOSL1-FZD7-PPP2CA	35591	32520	50960	44000	21144	
FZD8-GSK3A-PPP2CA	38405	48371	34300	29334	6995	CTNNB1P1-JUN-PPP2CA	1200	14488	18797	18145	43428	
CSNK1D-FOXN1-PPP2CA	18148	46116	27668	8407	45131	FBXW11-FOXN1-PPP2CA	19429	5233	11810	11471	27138	
FRZB-JUN-PPP2CA	7300	14667	7614	23131	10832	CSNK2A1-FOXN1-PPP2CA	9022	16430	12781	23632	52199	
PPP2CA-T-WNT3A	8306	15391	15440	22058	43691	FRZB-FZD2-PPP2CA	45767	45197	36507	39569	52662	
CSNK1G1-FSHB-PPP2CA	45864	55377	47231	36646	7302	CCND1-JUN-PPP2CA	23078	52819	9647	2403	50956	
CSNK2A1-FSHB-PPP2CA	8916	2500	542	374	35437	KREMEN1-PPP2CA-WNT2B	2599	25978	4343	22180	25119	
DKK1-FOXN1-PPP2CA	3888	47099	23168	15037	7506	FRZB-GSK3A-PPP2CA	38472	20495	45117	47106	5800	
BTRC-PPP2CA-WNT4	44520	22084	53956	47933	11904	FZD5-CCND3-PPP2CA	8115	1337	11428	7612	8874	
PPP2CA-WNT1-WNT4	8831	44953	16654	15477	52783	AES-FOXN1-PPP2CA	15552	17852	20538	20892	52165	
FZD8-PORCN-PPP2CA	19196	45384	18240	7276	44603	FZD5-PPP2CA-SFRP4	43148	2590	51212	53827	7773	
CSNK1A1-LRP6-PPP2CA	21805	35780	26361	19325	3996	FOSL1-NKD1-PPP2CA	2142	38096	5085	20731	35691	
FZD7-PPP2CA-WNT2B	49373	38171	36850	38963	35731	APC-BTRC-PPP2CA	22392	28302	364	23734	44217	
FOSL1-PORCN-PPP2CA	48261	18485	32801	52162	23392	FRZB-NKD1-PPP2CA	40960	47308	36156	34176	2451	
AXIN1-FZD2-PPP2CA	53993	12881	38050	33879	3565	DKK1-PPP2CA-SEN2	54912	42266	45187	36664	4020	
CSNK1D-FGF4-PPP2CA	45504	35247	32816	42764	13525	FZD8-JUN-PPP2CA	19614	7200	12631	7664	50841	
DKK1-NKD1-PPP2CA	56475	3125	43099	41619	4718	CSNK1G1-JUN-PPP2CA	49728	12194	55667	43794	1187	
FBXW11-JUN-PPP2CA	26696	20517	25233	5300	51847	FZD6-GSK3A-PPP2CA	47697	29555	40386	36698	423	
FOSL1-GSK3A-PPP2CA	1409	42580	3372	20682	38693	DAAM1-LRP6-PPP2CA	14753	15473	7995	19908	35471	
CSNK1A1-GSK3B-PPP2CA	49724	16745	29212	44256	8827	BCL9-JUN-PPP2CA	45740	3344	48124	47202	6677	
FRZB-PPP2CA-SFRP4	47312	32897	44586	44705	7631	CTBP2-FOXN1-PPP2CA	17323	28030	4898	5272	35257	
DKK1-GSK3A-PPP2CA	56171	44330	46143	47677	9774	BCL9-FGF4-PPP2CA	13108	47224	18028	10216	35400	
FRAT1-JUN-PPP2CA	14423	55965	18214	20111	55748	APC-PORCN-PPP2CA	26107	21082	3362	24620	44778	
CXXC4-FZD2-PPP2CA	48257	39680	46070	54823	47811	FRAT1-GSK3A-PPP2CA	35360	46417	34830	42562	36551	
BTRC-PPP2CA-SFRP4	48696	12060	50892	40797	32684	FRZB-PORCN-PPP2CA	27080	50041	23642	27870	37579	
EP300-FZD2-PPP2CA	26266	2702	16127	4968	42671	DAAM1-GSK3A-PPP2CA	43227	23087	42047	56405	591	
CCND3-PPP2CA-WNT2	36471	39248	32988	47293	15179	FBXW2-NKD1-PPP2CA	48789	9344	52507	46333	3977	
PITX2-PORCN-PPP2CA	48624	10701	36145	29228	15037	CTBP1-FOXN1-PPP2CA	25363	14039	7091	10247	30526	
FZD7-PPP2CA-WNT2	7778	19092	20329	18156	22398	CCND3-PPP2CA-SEN2	43161	29979	39622	44082	22425	
PPP2CA-WNT1-WNT5A	48329	11938	40478	41705	4471	AXIN1-FOXN1-PPP2CA	12206	47570	25201	11633	33808	
NKD1-PPP2CA-SFRP4	36127	4970	52255	56608	11433	FGF4-FOSL1-PPP2CA	2668	4065	11722	25274	53689	
AES-EP300-PPP2CA	27875	26880	13013	26533	45960	CTBP1-FGF4-PPP2CA	44789	15602	54942	51998	5614	
DIXDC1-FOXN1-PPP2CA	55813	13913	43667	51754	13189	APC-FOXN1-PPP2CA	27764	11028	6196	16202	43577	
CXXC4-FOXN1-PPP2CA	3477	1511	1989	21870	13869	CCND3-NKD1-PPP2CA	42363	24532	31404	38395	21255	
GSK3B-LRP6-PPP2CA	10854	12468	23233	9094	55175	FOSL1-JUN-PPP2CA	47425	55951	39423	37994	17117	
FBXW11-FZD2-PPP2CA	34671	38019	42105	37659	1783	FOSL1-PPP2CA-SFRP4	9922	2195	4478	5867	44367	
CXXC4-FGF4-PPP2CA	45268	56658	41145	41538	2318	CCND1-NKD1-PPP2CA	45411	49544	40077	44095	7701	
PPP2CA-TCF7-WNT3A	53743	13986	53761	54445	6921	FBXW2-PORCN-PPP2CA	23648	32647	9681	6402	43830	
AES-DVL1-PPP2CA	31643	25017	55574	39311	5215	CXXC4-JUN-PPP2CA	12942	55409	5351	11313	42743	
DIXDC1-FZD2-PPP2CA	5808	37464	22448	10828	35992	DAAM1-FGF4-PPP2CA	31686	7294	36347	45385	24985	
FZD8-NKD1-PPP2CA	44458	15474	35698	28867	8497	APC-FZD6-PPP2CA	45246	44200	51681	35207	3563	
FZD6-PORCN-PPP2CA	134	51933	21395	21054	54797	BTRC-PPP2CA-T	1966	5549	26054	18488	55393	
FBXW11-GSK3A-PPP2CA	39636	12964	49334	55696	4728	FZD5-PORCN-PPP2CA	16272	5440	27445	2373	50948	
CSNK2A1-NKD1-PPP2CA	35993	44148	33793	48908	1488	CSNK1D-GSK3A-PPP2CA	38964	24815	30788	42585	4984	
DIXDC1-PITX2-PPP2CA	53041	37364	46121	33605	10550	DKK1-DVL2-PPP2CA	48548	5136	42876	30513	25830	
FZD8-LEF1-PPP2CA	52178	12148	30523	45325	15015	FRAT1-PORCN-PPP2CA	16216	46645	23644	20053	49567	
CCND3-PPP2CA-RHOU	13938	26769	17584	13088	34833	CSNK2A1-GSK3A-PPP2CA	50785	50502	56753	49920	960	
PPP2CA-WNT1-WNT2B	39456	965	50325	49872	8953	FZD1-PORCN-PPP2CA	27029	44486	23937	16319	39532	
FZD7-PPP2CA-TLE2	54989	26286	31172	34581	24459	CTNNB1-GSK3A-PPP2CA	15830	21803	10476	3412	31907	
CCND1-CTNNB1P1-PPP2CA	24827	31527	22030	28201	34231	KREMEN1-PPP2CA-SEN2	56219	44163	55663	29787	8652	

Table 3: Rankings of PPP2CA-X-X. A list of approximately first 125 combinations with rankings below 10,000 out of 57,155. SA - SOBOL; Implementation - 2002

### 6.3.3. Examining the behaviour of BCL-PPP2CA-X combinations

Deng et al. [19] show that phosphorylation of BCL2 occurs rapidly after the addition of agonist to IL-3-deprived cells and can be reversed by the action of an okadaic acid (OA)-sensitive phosphatase. They make several observations that support the role for

RANKING @ $t_i$ USING SOBOL - MARTINEZ												
3rd order comb.	$t_1$	$t_3$	$t_6$	$t_{12}$	$t_{24}$	3rd order comb.	$t_1$	$t_3$	$t_6$	$t_{12}$	$t_{24}$	
CXXC4-FZD7-PPP2CA	36776	55789	52424	25177	54487	FZD7-PPP2CA-SFRP4	1497	55447	6371	5058	3337	
FZD1-FZD7-PPP2CA	1008	29279	12451	39499	50001	AES-AXIN1-PPP2CA	42020	40917	4324	34889	30000	
CSNK2A1-MYC-PPP2CA	641	3083	16208	54190	40209	APC-PITX2-PPP2CA	13736	5292	47096	11939	9629	
NLK-PORCN-PPP2CA	37331	14886	22559	45950	6790	PPP2CA-SFRP4-WNT2B	13418	45868	44709	51672	55851	
KREMEN1-PPP2CA-SFRP4	8033	44599	37769	50506	31645	FZD7-NKD1-PPP2CA	41077	46695	30291	56451	41703	
DKK1-JUN-PPP2CA	16976	18784	14132	11492	11442	BCL9-PORCN-PPP2CA	36593	35690	46380	55538	25115	
DIXDC1-NKD1-PPP2CA	5108	14247	10722	14891	52539	CXXC4-PORCN-PPP2CA	18980	12646	41076	17858	34882	
DVL2-JUN-PPP2CA	35923	8438	19130	28183	37748	FZD7-PPP2CA-SEN2	20018	21717	46184	2450	53554	
CCND3-PPP2CA-SFRP4	43450	35483	9097	11874	57031	PPP2CA-WNT1-WNT3A	51242	1279	28051	1456	15170	
DKK1-PPP2CA-SFRP4	17007	2236	25529	7435	54887	FBXW11-LRP6-PPP2CA	46810	13605	31979	34037	4479	
FSHB-FZD2-PPP2CA	20341	18178	13864	46410	55298	CSNK1G1-NKD1-PPP2CA	19784	21076	9213	14040	31099	
DVL1-FOXN1-PPP2CA	9766	3745	17308	8852	45843	DAAM1-FOXN1-PPP2CA	9163	6334	21471	16668	33204	
CTBP1-GSK3A-PPP2CA	26640	25404	46206	309	47538	FOSL1-FOXN1-PPP2CA	21982	3651	43234	19001	11166	
CSNK1G1-FZD2-PPP2CA	6902	15684	9374	21259	4565	FOSL1-FZD7-PPP2CA	7623	24057	41611	37347	7700	
FZD8-GSK3A-PPP2CA	10841	42433	6073	22129	10018	CTNNB1P1-JUN-PPP2CA	35131	50326	1387	2781	52171	
CSNK1D-FOXN1-PPP2CA	35792	53371	27044	46895	15279	FBXW11-FOXN1-PPP2CA	11800	8011	18604	2385	6113	
FRZB-JUN-PPP2CA	13541	57069	53146	52693	38925	CSNK2A1-FOXN1-PPP2CA	6777	56192	42475	44384	6122	
PPP2CA-T-WNT3A	21205	15120	48258	46762	44219	FRZB-FZD2-PPP2CA	55947	54028	38	2570	8523	
CSNK1G1-FSHB-PPP2CA	40612	43508	22826	3439	25861	CCND1-JUN-PPP2CA	42904	56795	22325	53788	5368	
CSNK2A1-FSHB-PPP2CA	18252	39529	48641	45395	6382	KREMEN1-PPP2CA-WNT2B	36014	45601	55143	6929	4063	
DKK1-FOXN1-PPP2CA	44706	20274	13997	48661	39549	FRZB-GSK3A-PPP2CA	44919	37114	8287	10635	8979	
BTRC-PPP2CA-WNT4	18544	53592	12219	41275	6887	FZD5-CCND3-PPP2CA	2762	57115	56278	39115	3562	
PPP2CA-WNT1-WNT4	45922	51703	31831	5639	9	AES-FOXN1-PPP2CA	29571	6238	7129	6374	55299	
FZD8-PORCN-PPP2CA	4362	22959	16034	3701	20999	FZD5-PPP2CA-SFRP4	46954	32076	37079	2111	46440	
CSNK1A1-LRP6-PPP2CA	42454	18402	25345	47495	4538	FOSL1-NKD1-PPP2CA	45879	24082	5855	50930	2635	
FZD7-PPP2CA-WNT2B	16737	33330	1637	33682	42332	APC-BTRC-PPP2CA	27066	7976	28250	12749	21392	
FOSL1-PORCN-PPP2CA	8604	37919	49115	19867	23808	FRZB-NKD1-PPP2CA	52371	40952	44274	55170	8712	
AXIN1-FZD2-PPP2CA	46267	45497	35341	27378	16395	DKK1-PPP2CA-SEN2	29022	2790	15842	29509	37949	
CSNK1D-FGF4-PPP2CA	55329	26273	1032	21669	55925	FZD8-JUN-PPP2CA	51520	6649	18580	11738	53314	
DKK1-NKD1-PPP2CA	33743	9918	7761	39827	40352	CSNK1G1-JUN-PPP2CA	52121	39360	27268	41319	22355	
FBXW11-JUN-PPP2CA	20877	54414	32670	38800	8762	FZD6-GSK3A-PPP2CA	30831	45120	42347	19249	34318	
FOSL1-GSK3A-PPP2CA	3591	33875	8900	36670	1652	DAAM1-LRP6-PPP2CA	40026	21133	39236	9647	42193	
CSNK1A1-GSK3B-PPP2CA	52426	31010	46086	43164	48650	BCL9-JUN-PPP2CA	19114	21036	47756	53352	38267	
FRZB-PPP2CA-SFRP4	50706	30998	2561	26713	8651	CTBP2-FOXN1-PPP2CA	35005	52494	40801	14342	52568	
DKK1-GSK3A-PPP2CA	36627	20670	30552	11028	29421	BCL9-FGF4-PPP2CA	3142	16747	11573	5963	13912	
FRAT1-JUN-PPP2CA	18796	55637	7251	29192	8902	APC-PORCN-PPP2CA	2836	3231	15247	16608	2574	
CXXC4-FZD2-PPP2CA	56822	40204	3700	13007	19199	FRAT1-GSK3A-PPP2CA	39172	41845	6227	25898	13956	
BTRC-PPP2CA-SFRP4	36763	46459	15211	1307	23454	FRZB-PORCN-PPP2CA	117	8687	53213	56391	54110	
EP300-FZD2-PPP2CA	8595	21744	56912	41698	6259	DAAM1-GSK3A-PPP2CA	52648	33200	25725	45375	19354	
CCND3-PPP2CA-WNT2	38632	30222	6158	16261	54799	FBXW2-NKD1-PPP2CA	11451	1927	41714	38264	27169	
PITX2-PORCN-PPP2CA	13665	21071	35213	8665	8832	CTBP1-FOXN1-PPP2CA	41122	42280	51365	15729	42775	
FZD7-PPP2CA-WNT2	9708	5993	16965	5318	3724	CCND3-PPP2CA-SEN2	47671	41803	9981	18785	56616	
PPP2CA-WNT1-WNT5A	51641	38045	26358	31132	12482	AXIN1-FOXN1-PPP2CA	930	41599	54345	42965	705	
NKD1-PPP2CA-SFRP4	7636	40918	29991	8329	13251	FGF4-FOSL1-PPP2CA	34076	11002	7176	22758	44026	
AES-EP300-PPP2CA	2675	16717	54436	50242	55608	CTBP1-FGF4-PPP2CA	25913	21812	39784	28223	8196	
DIXDC1-FOXN1-PPP2CA	35953	3598	11243	27761	42557	APC-FOXN1-PPP2CA	8301	1761	7313	14130	49333	
CXXC4-FOXN1-PPP2CA	32928	38757	46239	12285	33975	CCND3-NKD1-PPP2CA	44598	34434	5620	11985	55806	
GSK3B-LRP6-PPP2CA	13135	10941	42334	56337	37182	FOSL1-JUN-PPP2CA	9738	4179	49861	43749	38763	
FBXW11-FZD2-PPP2CA	35561	52974	27006	43001	29809	FOSL1-PPP2CA-SFRP4	46320	53153	21382	6794	3185	
CXXC4-FGF4-PPP2CA	55018	25356	52250	908	48805	CCND1-NKD1-PPP2CA	30462	2994	26006	982	37703	
PPP2CA-TCF7-WNT3A	33451	27979	41924	1311	22611	FBXW2-PORCN-PPP2CA	33315	52616	8739	11832	17398	
AES-DVL1-PPP2CA	21089	22231	35484	43895	35402	CXXC4-JUN-PPP2CA	19551	7263	1665	24659	22732	
DIXDC1-FZD2-PPP2CA	54976	12173	19646	34326	33129	DAAM1-FGF4-PPP2CA	18833	30583	46625	49378	30333	
FZD8-NKD1-PPP2CA	23391	14419	3617	33513	22490	APC-FZD6-PPP2CA	56925	30837	35125	46871	17160	
FZD6-PORCN-PPP2CA	24378	12304	24722	7809	10296	BTRC-PPP2CA-T	6893	28574	13996	11972	37713	
FBXW11-GSK3A-PPP2CA	56455	33	12596	51548	22435	FZD5-PORCN-PPP2CA	14141	29708	13984	6123	2013	
CSNK2A1-NKD1-PPP2CA	36783	42052	28232	9350	10631	CSNK1D-GSK3A-PPP2CA	49948	27496	4120	13149	30348	
DIXDC1-PITX2-PPP2CA	13451	49710	9306	15472	45623	DKK1-DVL2-PPP2CA	9538	20006	26092	54939	45166	
FZD8-LEF1-PPP2CA	29034	50876	13787	5814	17937	FRAT1-PORCN-PPP2CA	40340	33092	34294	8634	52771	
CCND3-PPP2CA-RHOU	20334	7769	53314	46711	32292	CSNK2A1-GSK3A-PPP2CA	53147	43418	27751	30515	14659	
PPP2CA-WNT1-WNT2B	40253	4960	32537	41490	12692	FZD1-PORCN-PPP2CA	1916	19905	52539	7319	48499	
FZD7-PPP2CA-TLE2	5422	33917	15146	18254	34916	CTNNB1-GSK3A-PPP2CA	51702	25973	21658	30868	45983	
CCND1-CTNNB1P1-PPP2CA	5771	14934	44368	17420	50662	KREMEN1-PPP2CA-SEN2	57112	54087	23877	18652	19715	

Table 4: Rankings of PPP2CA-X-X. A list of approximately first 125 combinations with rankings below 10,000 out of 57,155. SA - SOBOL; Implementation - martinez

PP2A as the BCL2 regulatory phosphatase: • dephosphorylation of BCL2 is blocked by OA, a potent PP1 and PP2A inhibitor; • intracellular PP2A, but not PP1, co-localizes with BCL2; • the purified PP2AC catalytic subunit directly dephosphorylates BCL2 in vitro in an OA-sensitive manner;  $\beta$  the purified PP2Ac catalytic subunit preferentially

dephosphorylates BCL2 in vitro compared with PP1 and PP2B; • reciprocal immunoprecipitation studies indicate a direct interaction between PP2A and hemagglutinin (HA)-BCL2; and • treatment of factor-deprived cells with bryostatin 1 dramatically increases the association between PP2A and BCL2. They propose functional phosphorylation of BCL2 at Ser<sup>70</sup> to be a dynamic process regulated by the sequential action of an agonist-activated BCL2 kinase and PP2A. Via quantitative phospho-proteomic analysis, Brewer et al. [10] identified BCL-9/9L to be substrate of PPP2CA.

Looking at the tables above, one finds the following combinations for members of BCL family along with PPP2CA, to be prominent at 3rd order level - BCL9-PORCN-PPP2CA, BCL9-JUN-PPP2CA and BCL9-FGF4-PPP2CA. All these combinations indicate the existence of a possible synergy when they take a higher rank in the list of combinations.

#### **6.3.4. Examining the behaviour of Cyclin-PPP2CA-X combinations**

Cyclin G2 (CCNG2), together with cyclin G1 (CCNG1) and cyclin I (CCNI), defines a novel cyclin family expressed in terminally differentiated tissues including brain and muscle. Bennin et al. [20] tested the hypothesis that CCNG2 may be a negative regulator of cell cycle progression and found that ectopic expression of CCNG2 induces the formation of aberrant nuclei and cell cycle arrest in HEK293 and Chinese hamster ovary cells. They determined that CCNG2 and its homolog CCNG1 directly interact with the catalytic subunit of PP2A. Further, the ability of CCNG2 to inhibit cell cycle progression correlates with its ability to bind PP2A/B' and C subunits. Together, their findings suggested that CCNG2-PP2A complexes inhibit cell cycle progression. Looking at the tables above, one finds the following combinations for members of cyclin (CCN) family along with PPP2CA, to be prominent at 3rd order level - CCND3-PPP2CA-SFRP4, CCND3-PPP2CA-WNT2, CCND3-PPP2CA-RHOU, CCND1-CTNNBIP1-PPP2CA, CCND1-JUN-PPP2CA, FZD5-CCND3-PPP2CA, CCND3-PPP2CA-SEN2, CCND3-NKD1-PPP2CA, and CCND1-NKD1-PPP2CA. All these combinations indicate the existence of a possible synergy when they take a higher rank in the list of combinations.

#### **6.3.5. Examining the behaviour of CSNK-PPP2CA-X combinations**

Casein kinase (CSNK) 1A (CK1A) functions as a pivotal negative regulator of WNT signaling pathway, initiating the events that destabilize  $\beta$ -catenin. Shen et al. [21] show that CK1A activity requires its association with PPP2CA on AXIN, the scaffold protein of the  $\beta$ -catenin destruction complex. They found that WNT stimulation induced the dissociation of PPP2CA from CK1A, which resulted in CK1A autophosphorylation and its consequent inactivation. Further, autophosphorylated CK1A was enriched in a subset of colorectal cancers (CRCs) harboring constitutive WNT activation. Their findings identified a mechanism by which WNT stimulation inactivates CK1A, thus filling a critical gap in understanding of WNT signaling, with relevance for CRC. Via quantitative phospho-proteomic analysis, Brewer et al. [10] identified CSNK-1D/1E/A1 to be substrate of PPP2CA.

Looking at the tables above, one finds the following combinations for members of CSNK family along with PPP2CA, to be prominent at 3rd order level - CSNK2A1-MYC-PPP2CA, CSNK1G1-FZD2-PPP2CA, CSNK1D-FOXN1-PPP2CA, CSNK1G1-FSHB-PPP2CA, CSNK2A1-FSHB-PPP2CA, CSNK1A1-LRP6-PPP2CA, CSNK1D-FGF4-PPP2CA, CSNK1A1-GSK3B-PPP2CA, CSNK2A1-NKD1-PPP2CA, CSNK1G1-NKD1-PPP2CA, CSNK2A1-FOXN1-PPP2CA, CSNK1G1-JUN-PPP2CA, CSNK1D-GSK3A-PPP2CA and CSNK2A1-GSK3A-PPP2CA. All these combinations indicate the existence of a possible synergy when they take a higher rank in the list of combinations.

### **6.3.6. Examining the behaviour of $\beta$ -catenin/CTNNB-PPP2CA-X combinations**

Yu et al. [22] show that a heat shock protein HSP105 is required for WNT signaling, since depletion of HSP105 compromises  $\beta$ -catenin concentration and target gene transcription upon WNT stimulation. Mechanistically, they found that HSP105 depletion disrupted the integration of PP2A into the  $\beta$ -catenin degradation complex, thus favoring the hyperphosphorylation and degradation of  $\beta$ -catenin. HSP105 was overexpressed in many types of tumors, thus correlating with increased nuclear  $\beta$ -catenin protein levels and WNT target gene upregulation. Via quantitative phosphoproteomic analysis, Brewer et al. [10] identified CTNNB1 to be substrate of PPP2CA. On the other hand Tago et al. [23] identified a novel catenin beta interacting protein 1 (CTNNBIP1 or ICAT) which inhibited the interaction of  $\beta$ -catenin with TCF-4 and repressed  $\beta$ -catenin/TCF-4-mediated transactivation. Furthermore, ICAT inhibited Xenopus axis formation by interfering with WNT signaling. It is not known if there is an interaction between PPP2CA and CTNNBIP1. Looking at the tables above, one finds the following combinations for CTNNBIP1 along with PPP2CA, to be prominent at 3rd order level - CCND1-CTNNBIP1-PPP2CA, CTNNBIP1-JUN-PPP2CA and CTNNB1-GSK3A-PPP2CA. All these combinations indicate the existence of a possible synergy when they take a higher rank in the list of combinations.

### **6.3.7. Examining the behaviour of GSK3-PPP2CA-X combinations**

Hyperphosphorylation of tau is pivotally involved in the pathogenesis of Alzheimer's disease (AD) and related tauopathies. Glycogen synthase kinase-3 $\beta$  (GSK3 $\beta$ ) and PP2A are crucial enzymes to regulate tau phosphorylation. Chu et al. [24] has previously reported the cross-talk between GSK3 $\beta$  and PP2A signaling and showed that PP2A could dephosphorylate GSK3 $\beta$  at Ser9. Chu et al. [24] investigated the dephosphorylation of GSK3 $\beta$  in brain extracts in the presence of phosphatase inhibitors and found that a PP2A-like phosphatase activity was required for dephosphorylation of GSK3 $\beta$  at Ser9. Further, they found that PP2A interacted with GSK3 $\beta$  and suppressed its Ser9 phosphorylation in vitro and in HEK-293FT cells. Activity of PP2A negatively correlated to the level of phosphorylated GSK-3 $\beta$  in kainic acid-induced excitotoxic mouse brain. Via quantitative phospho-proteomic analysis, Brewer et al. [10] identified GSK3-A/B to be substrate of PPP2CA.

Looking at the tables above, one finds the following combinations for members of GSK3 family along with PPP2CA, to be prominent at 3rd order level - CTBP1-

GSK3A-PPP2CA, FZD8-GSK3A-PPP2CA, FOSL1-GSK3A-PPP2CA, CSNK1A1-GSK3B-PPP2CA, DKK1-GSK3A-PPP2CA, GSK3B-LRP6-PPP2CA, FBXW11-GSK3A-PPP2CA, FRZB-GSK3A-PPP2CA, FZD6-GSK3A-PPP2CA, FRAT1-GSK3A-PPP2CA, DAAM1-GSK3A-PPP2CA, CSNK1D-GSK3A-PPP2CA, CSNK2A1-GSK3A-PPP2CA and CTNNB1-GSK3A-PPP2CA. All these combinations indicate the existence of a possible synergy when they take a higher rank in the list of combinations.

### **6.3.8. Examining the behaviour of JUN-PPP2CA-X combinations**

The proto-oncogene c-JUN is a component of activator protein-1 (AP1) transcription factor complexes that regulates processes essential for embryonic development, tissue homeostasis and malignant transformation. Induction of gene expression by c-JUN involves stimulation of its transactivation ability and upregulation of DNA binding capacity. Though it is well known that the c-JUN requires JNK-mediated phosphorylation of S63/S73, the mechanism(s) through which binding of c-JUN to its endogenous target genes is regulated remains poorly characterized. Gilan et al. [25] showed that interaction of c-JUN with chromatin is positively regulated by PP2A complexes targeted to c-JUN by the PR55 $\alpha$  regulatory subunit. PR55 $\alpha$ -PP2A specifically dephosphorylated T239 of c-JUN, thus promoting its binding to genes regulating tumour cell migration and invasion. Their findings suggested a critical role for interplay between JNK and PP2A pathways determining the functional activity of c-JUN/AP1 in tumour cells. Shi et al. [26] indicate that malignant fibrous histiocytoma amplified sequence 1 (MFHAS1) suppresses Toll-like receptor (TLR4) signaling pathway through induction of PP2AC subunit cytoplasm translocation and subsequent c-JUN degradation, leading finally to decrease AP1 activity and cytokines expression. Via quantitative phosphoproteomic analysis, Brewer et al. [10] identified JUN to be substrate of PPP2CA.

Looking at the tables above, one finds the following combinations for JUN along with PPP2CA, to be prominent at 3rd order level - DKK1-JUN-PPP2CA, DVL2-JUN-PPP2CA, FRZB-JUN-PPP2CA, FBXW11-JUN-PPP2CA, FRAT1-JUN-PPP2CA, CTNNBIP1-JUN-PPP2CA, CCND1-JUN-PPP2CA, FZD8-JUN-PPP2CA, CSNK1G1-JUN-PPP2CA, BCL9-JUN-PPP2CA, FOSL1-JUN-PPP2CA and CXXC4-JUN-PPP2CA. All these combinations indicate the existence of a possible synergy when they take a higher rank in the list of combinations.

### **6.3.9. Examining the behaviour of FOSL1-PPP2CA-X combinations**

Heterodimerization among the basic-leucine zipper (bZIP) proteins or among the basic-helixloop-helix-leucine zipper (bHLHZip) proteins confers a multitude of combinational activities to these transcription factors. While searching for cellular proteins which could directly interact with bHLHZip protein, USF, Pognonec et al. [27] found a bZIP protein, FRA1/FOSL1. Expression of exogenous USF led to a decrease in AP1-dependent transcription in F9 cells while co-expression of exogenous FRA1/FOSL1 restored the AP1 activity in a dose-dependent manner.

Further, the nuclear phosphoprotein c-JUN is a major component of the AP1 transcription factor, whose activity is augmented by many oncogenes. An important mechanism to stimulate AP1 function is N-terminal phosphorylation of c-JUN at the serine

residues 63 and 73 by the c-JUN N-terminal kinases (JNKs). To determine the function of c-JUN N-terminal phosphorylation (JNP) during oncogenic transformation in vitro and in vivo, Behrens et al. [28] used mice and cells harboring a mutant allele of c-JUN, which has the JNK phosphoacceptor serines changed to alanines (JUN-AA). JUN-AA immortalized fibroblasts expressing v-RAS and v-FOS showed reduced tumorigenicity in nude mice, but the efficiency of v-SRC transformation was unaffected by the lack of JNP. To assess the significance of JNP in tumour development in vivo, two transgenic mouse tumour models were employed. Skin tumour development caused by constitutive activation of the RAS pathway by K5-SOS-F expression and c-FOS-induced osteosarcoma formation were impaired in mice lacking JNP. Thus there is a connection between c-JUN and FOSL1, that might be existing. Finally, figure 4 in Clark and Ohlmeyer [29] shows c-JUN which combines with c-FOS and protein dephosphorylation is initiated by PP2A.

Looking at the tables above, one finds the following combinations for FOSL1 along with PPP2CA, to be prominent at 3rd order level - FOSL1-PORCN-PPP2CA, FOSL1-GSK3A-PPP2CA, FOSL1-FOXN1-PPP2CA, FOSL1-FZD7-PPP2CA, FOSL1-NKD1-PPP2CA, FGF4-FOSL1-PPP2CA, FOSL1-JUN-PPP2CA and FOSL1-PPP2CA-SFRP4. All these combinations indicate the existence of a possible synergy when they take a higher rank in the list of combinations.

### **6.3.10. Examining the behaviour of FOX-PPP2CA-X combinations**

PP2A is a tumour suppressor whose strong inhibition underlies the phosphorylation-dependent, anti-apoptotic mechanisms in chronic lymphocytic leukemia (CLL). Inactivation of PP2A is due to the cooperative action of the phosphorylation of Y307 of its catalytic subunit by the aberrant cytosolic pool of the SRC family kinase LYN and the interaction with its protein inhibitor SET, which is overexpressed in CLL. Pagano et al. [30] developed a library of compounds, the most potent being the one named CC11, which restores PP2A activity by disrupting the PP2A/SET complex, thereby triggering the mitochondrial pathway of apoptosis. They observe that this process involves the recruitment of the proapoptotic BH3-only proteins BAD and BIM to mitochondria, the former upon direct dephosphorylation and the latter being newly expressed upon dephosphorylation and activation of its transcription factor FOXO3A. Their findings highlighted that PP2A antagonized the prosurvival pathways controlled by AKT, which phosphorylates and thereby suppresses a variety of pro-apoptotic factors and tumour suppressors including BAD and FOXO3A. Looking at the tables above, one finds the following combinations for members of FOX family along with PPP2CA, to be prominent at 3rd order level - DVL1-FOXN1-PPP2CA, CSNK1D-FOXN1-PPP2CA, DKK1-FOXN1-PPP2CA, DIXDC1-FOXN1-PPP2CA, CXXC4-FOXN1-PPP2CA, DAAM1-FOXN1-PPP2CA, FOSL1-FOXN1-PPP2CA, FBXW11-FOXN1-PPP2CA, CSNK2A1-FOXN1-PPP2CA, AES-FOXN1-PPP2CA, CTBP2-FOXN1-PPP2CA, CTBP1-FOXN1-PPP2CA, AXIN1-FOXN1-PPP2CA and APC-FOXN1-PPP2CA. All these combinations indicate the existence of a possible synergy when they take a higher rank in the list of combinations.

### **6.3.11. Examining the behaviour of EP300-PPP2CA-X combinations**

Transcriptional coactivator p300 (or EP300) is required for embryonic development and cell proliferation. Valproic acid, a histone deacetylase inhibitor, is widely used in the therapy of epilepsy and bipolar disorder. Chen et al. [31] report that valproic acid stimulates proteasome-dependent p300 degradation through augmentation of gene expression of the B56 $\gamma$  regulatory subunits of protein phosphatase 2A. The B56 $\gamma$ 3 regulatory and catalytic subunits of protein phosphatase 2A interact with p300. Overexpression of the B56 $\gamma$ 3 subunit led to proteasome-mediated p300 degradation and repressed p300-dependent transcriptional activation, which required the B56 $\gamma$ 3 interaction domain of p300. Conversely, silencing of the B56 $\gamma$  subunit expression by RNA interference increased the stability and transcriptional activity of p300. Via quantitative phospho-proteomic analysis, Brewer et al. [10] identified EP300 to be substrate of PPP2CA.

Looking at the tables above, one finds the following combinations for Ep300 along with PPP2CA, to be prominent at 3rd order level - EP300-FZD2-PPP2CA and AES-EP300-PPP2CA. All these combinations indicate the existence of a possible synergy when they take a higher rank in the list of combinations.

## **7. Conclusion**

This manuscript studies the time behaviour of 3rd order combinations of PPP2CA in WNT3A stimulated HEK 293 cells. Based on the established 2nd order combinations of the PPP2CA, 3rd order combinations emerge using the machine learning based search engine. These 3rd order combinations might be of interest for further wet lab investigations.

## **Competing interests**

No competing interest is declared.

## **Author contributions statement**

SS conceived and designed the experiments; wrote the code; performed the experiments; analyzed the data; wrote the manuscript.

## **Availability of code**

Code for time series data available at CERN based Zenodo on <https://zenodo.org/records/14637456>.



## Acknowledgments

Special thanks to Mrs. Rita Sinha and late Mr. Prabhat Sinha for supporting the author financially, without which this work could not have been made possible.

## Supplementary

The following files (ending with .txt and can be opened in R or in simple text processing program) with these names are made available with this manuscript. For PPP2CA, (1) **-3-odr-TP-ranking-linear.txt**, (2) **-3-odr-TP-ranking-rbf.txt**, (3) **-3-odr-TP-ranking-2002.txt**, and (4) **-3-odr-TP-ranking-martinez.txt**, contain rankings for 3rd order combinations across each time point for, HSIC (linear kernel), HSIC (rbf kernel), SOBOL (2002 implementation) and SOBOL (martinez implementation), respectively.

## References

- [1] T. S. Gujral, G. MacBeath, A system-wide investigation of the dynamics of wnt signaling reveals novel phases of transcriptional regulation, *PloS one* 5 (2010) e10024.
- [2] S. Sinha, Machine learning ranking of plausible (un) explored synergistic gene combinations using sensitivity indices of time series measurements of wnt signaling pathway, *Integrative Biology* 16 (2024) zya020.
- [3] T. Joachims, Training linear svms in linear time, in: *Proceedings of the 12th ACM SIGKDD international conference on Knowledge discovery and data mining*, ACM, 2006, pp. 217–226.
- [4] Y. Shi, Serine/threonine phosphatases: mechanism through structure, *Cell* 139 (2009) 468–484.
- [5] Wikipedia contributors, Protein serine/threonine phosphatase — Wikipedia, the free encyclopedia, [https://en.wikipedia.org/w/index.php?title=Protein\\_serine/threonine\\_phosphatase&oldid=1226576715](https://en.wikipedia.org/w/index.php?title=Protein_serine/threonine_phosphatase&oldid=1226576715), 2024. [Online; accessed 6-March-2025].
- [6] T. Jones, H. Barker, E. Da Cruz e Silva, R. Mayer-Jaekel, B. Hemmings, N. Spurr, D. Sheer, P. Cohen, Localization of the genes encoding the catalytic subunits of protein phosphatase 2a to human chromosome bands 5q23-ζq31 and 8p12-ζp11. 2, respectively, *Cytogenetic and Genome Research* 63 (1993) 35–41.
- [7] P. Seshacharyulu, P. Pandey, K. Datta, S. K. Batra, Phosphatase: Pp2a structural importance, regulation and its aberrant expression in cancer, *Cancer letters* 335 (2013) 9–18.
- [8] S. Reynhout, V. Janssens, Physiologic functions of pp2a: Lessons from genetically modified mice, *Biochimica Et Biophysica Acta (BBA)-Molecular Cell Research* 1866 (2019) 31–50.
- [9] B. Hoermann, T. Kokot, D. Helm, S. Heinzlmeir, J. E. Chojnacki, T. Schubert, C. Ludwig, A. Berteotti, N. Kurzawa, B. Kuster, et al., Dissecting the sequence determinants for dephosphorylation by the catalytic subunits of phosphatases pp1 and pp2a, *Nature Communications* 11 (2020) 3583.
- [10] A. Brewer, G. Sathe, B. E. Pflug, R. G. Clarke, T. J. Macartney, G. P. Sapkota, Mapping the substrate landscape of protein phosphatase 2a catalytic subunit ppp2ca, *Iscience* 27 (2024).
- [11] S. Sinha, Hilbert-schmidt and sobol sensitivity indices for static and time series wnt signaling measurements in colorectal cancer-part a, *BMC systems biology* 11 (2017) 120.
- [12] S. Da Veiga, Global sensitivity analysis with dependence measures, *Journal of Statistical Computation and Simulation* 85 (2015) 1283–1305.

- [13] A. Saltelli, Making best use of model evaluations to compute sensitivity indices, *Computer physics communications* 145 (2002) 280–297.
- [14] J. Martinez, Analyse de sensibilité globale par décomposition de la variance, *Presentation in Journée des GdR Ondes & Mascot* 13 (2011) 207.
- [15] M. Baudin, K. Boumhaout, T. Delage, B. Iooss, J.-M. Martinez, Numerical stability of sobol’ indices estimation formula, in: *Proceedings of the 8th International Conference on Sensitivity Analysis of Model Output (SAMO 2016)*, volume 30, 2016, pp. 50–51.
- [16] K. Willert, S. Shibamoto, R. Nusse, Wnt-induced dephosphorylation of axin releases  $\beta$ -catenin from the axin complex, *Genes & development* 13 (1999) 1768–1773.
- [17] S. Ikeda, M. Kishida, Y. Matsuura, H. Usui, A. Kikuchi, Gsk-3 $\beta$ -dependent phosphorylation of adenomatous polyposis coli gene product can be modulated by  $\beta$ -catenin and protein phosphatase 2a complexed with axin, *Oncogene* 19 (2000) 537–545.
- [18] J. M. Seeling, J. R. Miller, R. Gil, R. T. Moon, R. White, D. M. Virshup, Regulation of  $\beta$ -catenin signaling by the b56 subunit of protein phosphatase 2a, *Science* 283 (1999) 2089–2091.
- [19] X. Deng, T. Ito, B. Carr, M. Mumby, W. S. May, Reversible phosphorylation of bcl2 following interleukin 3 or bryostatin 1 is mediated by direct interaction with protein phosphatase 2a, *Journal of Biological Chemistry* 273 (1998) 34157–34163.
- [20] D. A. Bennis, A. S. A. Don, T. Brake, J. L. McKenzie, H. Rosenbaum, L. Ortiz, A. A. DePaoli-Roach, M. C. Horne, Cyclin g2 associates with protein phosphatase 2a catalytic and regulatory b’ subunits in active complexes and induces nuclear aberrations and a g1/s phase cell cycle arrest, *Journal of Biological Chemistry* 277 (2002) 27449–27467.
- [21] C. Shen, W. Lu, S. B. Merugu, A. Bharti, S. M. Afify, L. Schnitkey, D. T. Wynn, F. Yang, T. M. Rohwetter, A. Nayak, et al., Wnt signaling inhibits casein kinase 1 $\alpha$  activity by modulating its interaction with protein phosphatase 2a, *Cell Reports* 44 (2025).
- [22] N. Yu, M. Kakunda, V. Pham, J. R. Lill, P. Du, M. Wongchenko, Y. Yan, R. Firestein, X. Huang, Hsp105 recruits protein phosphatase 2a to dephosphorylate  $\beta$ -catenin, *Molecular and cellular biology* 35 (2015) 1390–1400.
- [23] K.-i. Tago, T. Nakamura, M. Nishita, J. Hyodo, S.-i. Nagai, Y. Murata, S. Adachi, S. Ohwada, Y. Morishita, H. Shibuya, et al., Inhibition of wnt signaling by icat, a novel  $\beta$ -catenin-interacting protein, *Genes & development* 14 (2000) 1741–1749.
- [24] D. Chu, J. Tan, S. Xie, N. Jin, X. Yin, C.-X. Gong, K. Iqbal, F. Liu, Gsk-3 $\beta$  is dephosphorylated by pp2a in a leu309 methylation-independent manner, *Journal of Alzheimer’s Disease* 49 (2016) 365–375.
- [25] O. Gilan, J. Diesch, M. Amalia, K. Jastrzebski, A. C. Chueh, N. M. Verrills, R. B. Pearson, J. M. Mariadason, E. Tulchinsky, R. D. Hannan, et al., Pr55 $\alpha$ -containing protein phosphatase 2a complexes promote cancer cell migration and invasion through regulation of ap-1 transcriptional activity, *Oncogene* 34 (2015) 1333–1339.
- [26] Q. Shi, B. Xiong, J. Zhong, H. Wang, D. Ma, C. Miao, Mfhas1 suppresses tlr4 signaling pathway via induction of pp2a c subunit cytoplasm translocation and inhibition of c-jun dephosphorylation at thr239, *Molecular Immunology* 88 (2017) 79–88.
- [27] P. Pognonec, K. E. Boulukos, C. Aperlo, M. Fujimoto, H. Ariga, A. Nomoto, H. Kato, Cross-family interaction between the bhlhzip usf and bzip fra1 proteins results in down-regulation of ap1 activity, *Oncogene* 14 (1997) 2091–2098.
- [28] A. Behrens, W. Jochum, M. Sibilila, E. F. Wagner, Oncogenic transformation by ras and fos is mediated by c-jun n-terminal phosphorylation, *Oncogene* 19 (2000) 2657–2663.
- [29] A. R. Clark, M. Ohlmeyer, Protein phosphatase 2a as a therapeutic target in inflammation and neurodegeneration, *Pharmacology & therapeutics* 201 (2019) 181–201.
- [30] M. A. Pagano, E. Tibaldi, P. Molino, F. Frezzato, V. Trimarco, M. Facco, G. Zagotto, G. Ribaldo, L. Leanza, R. Peruzzo, et al., Mitochondrial apoptosis is induced by alkoxy phenyl-1-propanone derivatives through pp2a-mediated dephosphorylation of bad and foxo3a in cll, *Leukemia* 33 (2019) 1148–1160.
- [31] J. Chen, J. R. St-Germain, Q. Li, B56 regulatory subunit of protein phosphatase 2a mediates valproic acid-induced p300 degradation, *Molecular and cellular biology* 25 (2005) 525–532.